www.lajss.org
Latin American Journal of Solids and Structures 6 (2009) 105–129

Non axisymmetric free vibration analysis of linearly varying thickness shells of revolution by a bi-hierarchical finite element

Mohammed Nabil Ouissi[1,*] and Abderrahim Houmat[2]

[1]Laboratoire eau et ouvrages dans leurs environnements, University of Abou Bekr Belkad - Tlemcen Algeria
[2]Laboratoire d'automatique, University of Abou Bekr Belkad - Tlemcen Algeria

Abstract

A bi-hierarchical four nodes quadrilateral element with three displacements as degrees of freedom by node is developed to analyze the free vibration of isotropic shells of revolution with linearly varying thickness. The element is bi-hierarchical because of the double increase of the hierarchical mode number independently according to both axial and radial directions. The accuracy of solution is for high ratio dimensions as well flattened axisymmetric (plates) shells that slim ones (high cylindrical shells) with different shapes and boundary conditions. The second advantage is the possibility of using only one element to idealize composed shells of linearly varying thickness. Through the application of this element to some numerical examples, the comparisons with other studies show clearly that this element gives good results accuracy with simple idealization for axisymmetric and non-axisymmetric shells vibration (thick and thin).

Keywords: Bi-hierarchical finite element, double hierarchical increment, shells of revolution, linearly varying thickness, non – axisymmetric, free vibration.

1 Introduction

In this study, the non axisymmetric free vibration of linearly varying thickness isotropic shells of revolution is analyzed by using a new bi-hierarchical finite element. Shells of revolution of linearly varying thickness can be of different shape and dimensions, cylindrical, plate, thin or thick. In the standard finite element method or in the p-version, these shells can not be idealized by the same finite elements. The geometrical characteristics of the shell influence on the choice of the finite element and the mesh. To model for example a tank wall and its roof, one must have two elements, one for the wall and the other for the roof. The new proposed element can idealize the two shells.

The literature on finite element approximation of shells of revolution with linearly varying thickness is huge. Some approaches are mention here.

*Corresp. author email: ouissi_n@yahoo.fr Received 26 Dec 2008; In revised form 5 May 2009

An exact method [10], based on the development in power series, was used to solve the problems of free vibration of noncircular cylindrical shells having a circumferential thickness variation. In the study of the free vibrations of truncated conical shells of rotation of slightly varying thicknesses with annular strengthening [5], a solution was built up on the basis of linear shell and bar theory using the Ritz method.

To predict the natural frequencies of shells of revolution which may have arbitrary shape of meridian, general type of material property and any kind of boundary condition, a substructuring analysis method was presented in [13]. The method was developed in the context of first order shear deformation shell theory as well as the classical thin shell theory.

Other methods were implemented including a three-dimensional method to determine the frequencies and eigen modes of hollow bodies of revolution with arbitrary shell curvatures and arbitrarily varying curvatures [8]. A three-dimensional shell theory applicable to doubly curved thick open shell which are arbitrarily deep in one principal direction but are shallow in the other one, used Ritz variational formulation with algebraic polynomials as trial functions to extract the natural frequencies [14]. Solid and hollow hemi-ellipsoids of revolution (the hollow ones being shells) with and without an axially circular cylindrical hole [9], parabolod solids and parabolod shells of revolution with variable thickness [6], thick and complete (not truncated) conical shells of revolution [9] and hyperboloid shells of revolution [6] were analyzed by methods based on the 3-D dynamic equations of elasticity. The Ritz method was used to solve the eigenvalue problem.

A variety of finite elements was presented for shells of revolution of varying thickness such as the linear truncated elements based on the Kirchhoff's theory and the truncated elements with double curve based on the Mindlin – Reissner's theory [2]. The truncated elements are either with two displacements and one rotation by node, three displacements and one rotation, or for the not-axisymmetric case with three displacements and one rotation.

This study gives the possibility to idealize the majority of shells of revolution by only one element.

In the present paper, the proposed element is a four nodes volumetric and axisymmetric bi-hierarchical finite element with only displacements as degrees of freedom. The word "bi-hierarchical" comes from the fact that this element has two hierarchical mode numbers, one in the axis direction and the second in the radius one.

The two hierarchical mode numbers increase independently. This element can than idealize flattened shells as plates, high shells, as cylinders, and conical shells (thin and thick) or structures composed by them. For the first kind of shells, the radial direction hierarchical mode number is increased to get the the results' accuracy, and for the second kind, the axis hierarchical mode number is increased.

This element gives the possibility of reducing the mesh. The accuracy is not given by a high number of elements but only by increasing the two hierarchical mode numbers. Shells of revolution are of different kinds, shapes, thickness and boundary conditions. An axisymmetric structure composed of shells of revolution with constant or linearly varying thickness can be also idealized by only one finite element. The shape displacement is defined by a double hierarchical

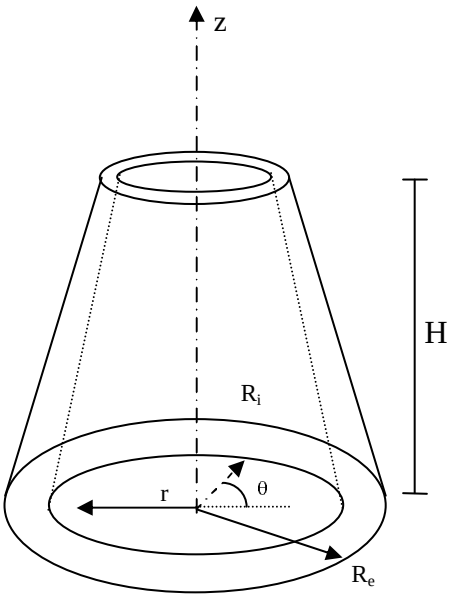

Figure 1: Shell of revolution with linearly varying thickness

increment.

2 Formulations

2.1 Potential energy

The potential energy stored in the shell is in the form of a strain energy due to the effect of both stretching and bending. The strain energy expression can be written as

$$U(t) = \frac{1}{2}\int_{R_i}^{R_e}\int_{0}^{H}\int_{0}^{2\pi}\left(\sigma_r\epsilon_r + \sigma_z\epsilon_z + \sigma_\theta\epsilon_\theta + \tau_{rz}\gamma_{rz} + \tau_{r\theta}\gamma_{r\theta} + \tau_{z\theta}\gamma_{z\theta}\right).r.dr.dz.d\theta z \qquad (1)$$

And in matrix form

$$U(t) = \frac{1}{2}\int\int\int\left(\{\epsilon\}^T.\{\sigma\}\right).r.dr.dz.d\theta \qquad (2)$$

where

$$\{\epsilon\} = \begin{Bmatrix} \epsilon_r \\ \epsilon_z \\ \epsilon_\theta \\ \gamma_{rz} \\ \gamma_{r\theta} \\ \gamma_{z\theta} \end{Bmatrix} \quad \text{and} \quad \{\sigma\} = \begin{Bmatrix} \sigma_r \\ \sigma_z \\ \sigma_\theta \\ \tau_{rz} \\ \tau_{r\theta} \\ \tau_{z\theta} \end{Bmatrix} \tag{3}$$

are the stain and stress vectors

The constitutive relationship between stress and strain is the generalized Hooke's law. For an isotropic homogeneous structure, it is given as

$$\{\sigma\} = [D] \,.\, \{\epsilon\} \tag{4}$$

Where $[D]$ is the elasticity matrix given by

$$[D] = E_1. \begin{bmatrix} 1-v & v & v & 0 & 0 & 0 \\ v & 1-v & v & 0 & 0 & 0 \\ v & v & 1-v & \frac{1-2v}{2} & 0 & 0 \\ 0 & 0 & 0 & 0 & \frac{1-2v}{2} & 0 \\ 0 & 0 & 0 & 0 & 0 & \frac{1-2v}{2} \end{bmatrix} \tag{5a}$$

where

$$E_1 = \frac{E}{(1+v) \,.\, (1-2v)} \tag{5b}$$

E is Young's modulus, and ν is Poisson ratio of the structure.

Substituting Eq. (4) into Eq. (2), the potential energy is given in terms of strain as

$$U\,(t) = \frac{1}{2} \int \int \int \left(\{\epsilon\}^T \,.\, [D] \,.\, \{\epsilon\} \right) .r.dr.dz.d\theta \tag{6}$$

The strain-displacement relations are given by

$$\{\epsilon\} = \left\{ \begin{array}{c} \epsilon_r \\ \epsilon_z \\ \epsilon_\theta \\ \gamma_{rz} \\ \gamma_{r\theta} \\ \gamma_{z\theta} \end{array} \right\} = \left\{ \begin{array}{c} \frac{\partial u}{\partial r} \\ \\ \frac{\partial v}{\partial z} \\ \\ \frac{u}{r} + \frac{1}{r} \cdot \frac{\partial w}{\partial \theta} \\ \\ \frac{\partial u}{\partial z} + \frac{\partial v}{\partial r} \\ \\ \frac{1}{r} \cdot \frac{\partial u}{\partial \theta} + \frac{\partial w}{\partial r} - \frac{w}{r} \\ \\ \frac{1}{r} \cdot \frac{\partial v}{\partial \theta} + \frac{\partial w}{\partial z} \end{array} \right\} \tag{7}$$

The strain vector can be expressed in term of the displacement vector as follows

$$\{\epsilon\} = [d] \,.\, \{\delta\} \tag{8}$$

where

$$\{\delta\} = \{u, v, w\} \tag{9}$$

and $[d]$ is a differential operator matrix defined by

$$\{d\} = \left[\begin{array}{ccc} \frac{\partial}{\partial r} & 0 & 0 \\ \\ 0 & \frac{\partial}{\partial z} & 0 \\ \\ \frac{1}{r} & 0 & \frac{1}{r} \cdot \frac{\partial}{\partial \theta} \\ \\ \frac{\partial}{\partial z} & \frac{\partial}{\partial r} & 0 \\ \\ \frac{1}{r} \cdot \frac{\partial}{\partial \theta} & 0 & \frac{\partial}{\partial r} - \frac{1}{r} \\ \\ 0 & \frac{1}{r} \cdot \frac{\partial}{\partial \theta} & \frac{\partial}{\partial z} \end{array} \right] \tag{10}$$

The stress vector can be expressed in terms of the displacement vector, as

$$\{\sigma\} = E_1. \begin{Bmatrix} (1-v).\frac{\partial u}{\partial r} + v.\left(\frac{\partial v}{\partial z} + \frac{u}{r} + \frac{1}{r}.\frac{\partial w}{\partial \theta}\right) \\ (1-v).\frac{\partial v}{\partial z} + v.\left(\frac{\partial u}{\partial r} + \frac{u}{r} + \frac{1}{r}.\frac{\partial w}{\partial \theta}\right) \\ (1-v).\left(\frac{u}{r} + \frac{1}{r}.\frac{\partial w}{\partial \theta}\right) + v.\left(\frac{\partial u}{\partial r} + \frac{\partial v}{\partial z}\right) \\ \frac{1-2v}{2}.\left(\frac{\partial u}{\partial z} + \frac{\partial v}{\partial r}\right) \\ \frac{1-2v}{2}.\left(\frac{1}{r}.\frac{\partial u}{\partial \theta} + \frac{\partial w}{\partial r} - \frac{w}{r}\right) \\ \frac{1-2v}{2}.\left(\frac{1}{r}.\frac{\partial v}{\partial \theta} + \frac{\partial w}{\partial z}\right) \end{Bmatrix} \tag{11}$$

2.2 Kinetic Energy

The kinetic energy of the shell can be written as

$$T(t) = \frac{1}{2}\int_{R_i}^{R_e}\int_0^H\int_O^{2\pi} \rho.\left[\left(\frac{\partial u(r,z,\theta,t)}{\partial t}\right)^2 + \left(\frac{\partial v(r,z,\theta,t)}{\partial t}\right)^2 + \left(\frac{\partial w(r,z,\theta,t)}{\partial t}\right)^2\right].r.dr.dz.d\theta \tag{12}$$

where, ρ is the density. Equation 12 can be written as follows

$$T(t) = \frac{1}{2}\int\int\int \rho.\left\{\dot{\delta}\right\}^T.\left\{\dot{\delta}\right\}.r.dr.dz.d\theta \tag{13}$$

where, $\{\delta\}$ is the displacement vector defined by Eq. (9) and, differentiation is with respect to the time, t.

2.3 Hierarchical Finite Element Formulation

The hierarchical finite element method known as the p-version of the finite element method is more precise and its convergence is faster than that of the h-method. Indeed, when the exact solution is analytical everywhere the rate of convergence is exponential, whereas that of the h-method is only algebraic. The quality of the solutions is not very sensitive to the distortions of the elements, which allows the use of flattened elements or great ratio on sides without penalizing the precision too much. In addition, as a hierarchical formulation is adopted for the representation of displacements, the matrix of stiffness relative to a given degree imbricates those of lower degrees. This makes it possible to obtain in an economic way a sequence of solutions instead of only one solution as in the case of the h-method [1, 11, 12].

The hp version of the finite element method has the characteristic to increase the precision by increasing both the interpolation polynomial degree and the number of finite elements as for the standard finite element method [11].

2.3.1 Idealization of the shell

The shell is divided into four nodes hierarchical axisymmetric quadrilateral isoparametric finite elements (see Fig.3). The element size is arbitrary, they may all be of the same size or may all be different. The shell can also be idealized by only one element if the thickness of the shell is varying linearly or if it is constant.

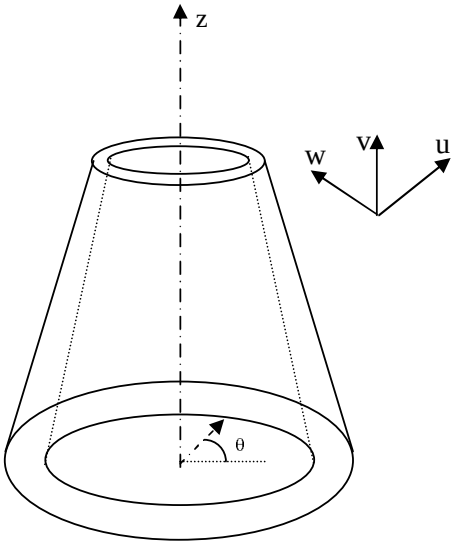

Figure 2: Displacements of a shell point

The axisymmetric free vibration of a shell of revolution which is a extension in the radial direction do not depend of the circumferential wave number n. However, for the non axisymmetric vibration, the natural free lateral vibrational modes of a circular cylindrical shell can be classified as the cosθ-type modes for which there is a single cosine wave of deflection in the circumferential direction, and as the cos$n\theta$-type modes for which the deflection of the shell involves a number of circumferential waves higher than 1. Figure 3 illustrates the circumferential and the vertical nodal patterns of these modes. For a tall cylindrical shell, the cos$n\theta$-type modes can be denoted beam-type modes because the shell behaves like a vertical cantilever beam.

The non axisymmetric free vibration of a shell being dependent of the circumferential wave number n, the equation of motion of the shell admit the representation of the radial, circumferential and axial displacement components u, v, and w (see Fig. 2) following respectively R, Z and θ in the following form

$$\begin{cases} u\left(r,z,\theta\right) = \bar{u}\left(r,z\right).\cos n\theta \\ v\left(r,z,\theta\right) = \bar{v}\left(r,z\right).\cos n\theta \\ w\left(r,z,\theta\right) = \bar{w}\left(r,z\right).\sin n\theta \end{cases} \tag{14}$$

where n is the circumferential wave number. The time dependence is removed by assuming

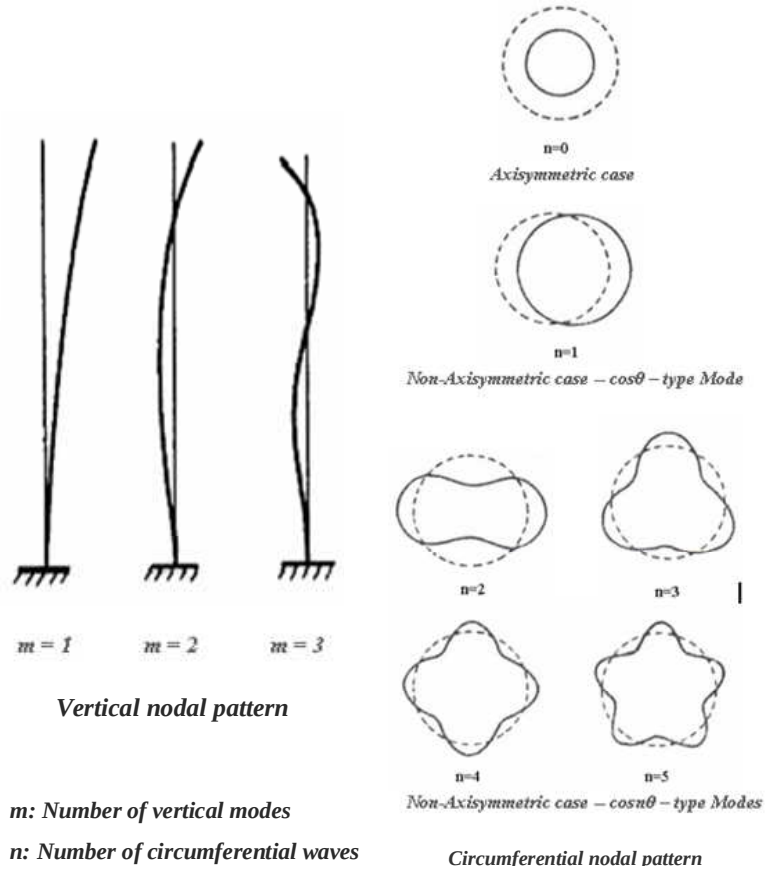

Figure 3: Shell vibration modes

that the displacements vary sinusodally in phase at the same frequency. The displacement functions $\bar{u}(r,z)$, $\bar{v}(r,z)$ and $\bar{w}(r,z)$ can be expressed in terms of the nodal displacements of the finite elements by means of an appropriate set of interpolation functions.

2.3.2 Shape Functions Selection

The hierarchical shape functions are generally selected in the Serendipity space. In this paper, the shape functions are built from the shifted Legendre orthogonal polynomials introduced by A. Houmat [3]. These polynomials are defined in the interval [0,1].

They can be classified in three categories

- Nodal shape functions
- Side shape functions
- Internal shape functions

Their recurring form is

$$\begin{cases} f_i(x) = 1 - x \\ f_i(x) = x \\ f_{i+2}(x) = \int_0^x P_i(\alpha)\,.d\alpha \end{cases} \tag{15}$$

where $P_i(\alpha)$ are the shifted Legendre polynomials defined by

$$\begin{cases} P_0(\alpha) = 1 \\ P_1(\alpha) = 2.\alpha - 1 \\ P_{i+1}(\alpha) = \frac{1}{i+1} \cdot \begin{bmatrix} (-2i - 1 + (4i+2)\alpha). \\ P_i(\alpha) - i \cdot P_{i+1}(\alpha) \end{bmatrix} \end{cases} \tag{16}$$

where i =1, 2, 3 ...

The shape functions are given on the basis of one-dimensional hierarchical finite element. The origin of the non-dimensional coordinates is at the left end of the element. For the C° continuous problems, the first two linear shape functions of the standard finite element method are retained. The higher order C° shape functions vanish at each end of the elements; they are used to describe the displacement function inside the element. These functions are generated by using the recursive formula 16.

$$\begin{cases} \bar{u}(r,z) = \sum_1^M N_i(r,z)\,.u_i \\ \bar{v}(r,z) = \sum_1^M N_i(r,z)\,.v_i \\ \bar{w}(r,z) = \sum_1^M N_i(r,z)\,.w_i \end{cases} \tag{17}$$

where

$$N_i(r,z) = f_k(r)\,.g_l(z) \tag{18}$$

with: k = 1,..,p+1 and l = 1,..,q+1
M = (p+1)(q+1)
p: Hierarchical mode number according to ξ
q: Hierarchical mode number according to η
f, g: Shape functions
The matrix form of the expression (17) is

$$\{\bar{\delta}\} = [N]\,.\,\{q\} \tag{19}$$

The first six hierarchical shape functions are represented in table 1.

Table 1: The first six hierarchical shape functions

$1-\xi$	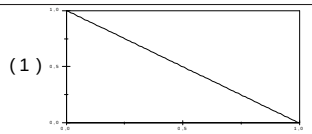
ξ	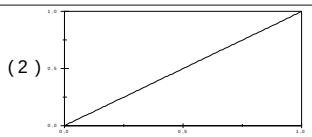
$\xi^2-\xi$	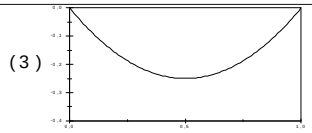
$2\xi^3-3\xi^2+\xi$	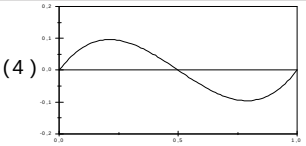
$5\xi^4-10\xi^3+$ $6\xi^2-\xi$	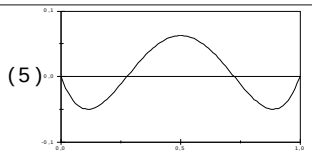
$14\xi^5-35\xi^4+$ $30\xi^3-10\xi^2+\xi$	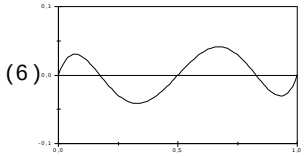

where

$$\{\bar{\delta}\} = \left\{ \begin{array}{l} \bar{u}\,(r,z) \\ \bar{v}\,(r,z) \\ \bar{w}\,(r,z) \end{array} \right\} \tag{20}$$

is the generalized displacement vector,

$$\{q\} = \{u_1, v_1, w_1, \ldots, u_i, v_i, w_i, \ldots\}^T \tag{21}$$

with i=1,...,$(p+1)(q+1)$
is the nodal displacement vector, and

$$[N] = \left\lfloor [N_1], [N_2], \ldots, [N_i], \ldots, \left\lfloor N_{(p+1)(q+1)} \right\rfloor \right\rfloor \tag{22}$$

is the shape function matrix, where $[N_i]$ is a sub-matrix given by

$$[N_i] = \begin{bmatrix} f_k(r).g_l(z) & 0 & 0 \\ 0 & f_k(r).g_l(z) & 0 \\ 0 & 0 & f_k(r).g_l(z) \end{bmatrix} \tag{23}$$

$f_k(r)$ and $g_l(z)$ are the nodal, side and internal shape functions of the element.

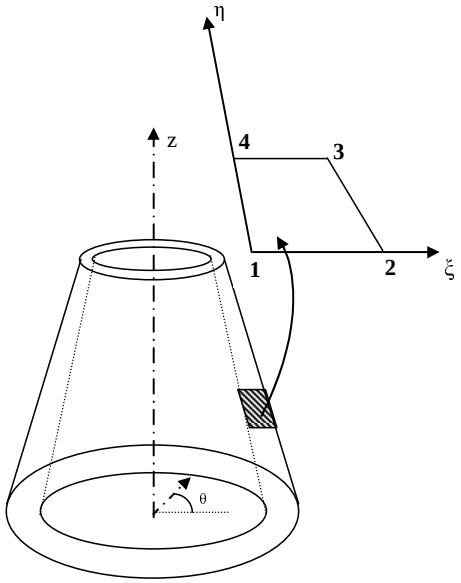

Figure 4: Cylindrical and non-dimensional coordinates

2.3.3 Shell Stiffness Matrix

The definition of the shell stiffness is reduced to the evaluation of the stiffness of a typical element. Expression (14) can be written

$$\{\delta\} = [\theta_n] . \left\{\bar{\delta}\right\} \tag{24}$$

where

$$[\theta_n] = \begin{bmatrix} \cos n\,\theta & 0 & 0 \\ 0 & \cos n\,\theta & 0 \\ 0 & 0 & \sin n\,\theta \end{bmatrix} \tag{25}$$

Substituting Eq. 24 into Eq. 8, then one can write

$$\{\varepsilon\} = [d]\{\delta\} = [d][\theta_n]\left\{\bar{\delta}\right\} = \left\lfloor \bar{d} \right\rfloor \left\{\bar{\delta}\right\} \tag{26}$$

where

$$\left[\bar{d}\right] = \begin{bmatrix} \frac{\partial}{\partial r}\cos n\,\theta & 0 & 0 \\ 0 & \frac{\partial}{\partial z}\cos n\,\theta & 0 \\ \frac{1}{r}\cos n\,\theta & 0 & \frac{n}{r}\cos n\,\theta \\ \frac{\partial}{\partial z}\cos n\,\theta & \frac{\partial}{\partial r}\cos n\,\theta & 0 \\ -\frac{n}{r}\sin n\,\theta & 0 & \left(\frac{\partial}{\partial r}-\frac{1}{r}\right)\sin n\,\theta \\ 0 & -\frac{n}{r}\sin n\,\theta & \frac{\partial}{\partial z}\sin n\,\theta \end{bmatrix} \tag{27}$$

Substituting Eq. 26 into Eq. 6, the potential energy can be written as

$$U(t) = \frac{1}{2}\int_{R_i}^{R_e}\int_0^H\int_0^{2\pi}\left(\left(\left[\bar{d}\right].\left\{\bar{\delta}\right\}\right)^T.[D].\left[\bar{d}\right].\left\{\bar{\delta}\right\}\right).r.dr.dz.d\theta \tag{28}$$

To evaluate the stiffness matrix of an element, the global cylindrical coordinates (r, z) may be expressed in terms of the local dimensionless coordinates (ξ, η) by

$$\begin{cases} r = (1-\xi).(1-\eta).r_1 + \xi.(1-\eta)\,r_2 + \xi.\eta.r_3 + (1-\xi).\eta.r_4 \\ z = (1-\xi).(1-\eta).z_1 + \xi.(1-\eta)\,z_2 + \xi.\eta.z_3 + (1-\xi).\eta.z_4 \end{cases} \tag{29}$$

where r_i and z_i are the cylindrical coordinates of the element nodes.

The coordinates ξ and η used to define the element geometry are given by the figure 4. They are varying from 0 to 1 whose origin is the node lower right of the element.

The derivatives can be written using the Jacobian matrix

$$\begin{Bmatrix} \frac{\partial}{\partial\xi} \\ \frac{\partial}{\partial\eta} \end{Bmatrix} = [J].\begin{Bmatrix} \frac{\partial}{\partial r} \\ \frac{\partial}{\partial z} \end{Bmatrix} \tag{30a}$$

where

$$[J] = \begin{bmatrix} \frac{\partial r}{\partial\xi} & \frac{\partial z}{\partial\xi} \\ \frac{\partial r}{\partial n} & \frac{\partial z}{\partial\eta} \end{bmatrix} \tag{30b}$$

And then after mathematical transformations, one can write

$$r.dr.dz.d\theta = k.\pi.|J|.r.d\xi.d\eta \tag{31}$$

Where k = 2 for n = 0 and k = 1 for n = 1,2,... (n: circumferential wave number).

n is the circumferential wave number and $|J|$ is the Jacobian matrix.

Substituting Eqs. 31 and 19 into Eq. 28, the potential energy can be written, as

$$\begin{aligned} U(t) &= \frac{k\pi}{2}\int_0^1\int_0^1 \left(\{q\}^T.[N]^T.\left[\bar{d}\right]^T.[D].\left[\bar{d}\right].[N].\{q\}\right).|J|.r.d\xi.dn && (32a)\\ &= \frac{1}{2}\{q\}^T.\left[k\pi.\int_0^1\int_0^1 \left(.[N]^T\left[\bar{d}\right]^T.[D].\left[\bar{d}\right].[N].\right).|J|.r.d\xi.d\eta\right].\{q\} && (32b)\\ &= \frac{1}{2}\{q\}^T.[K].\{q\} && (32c) \end{aligned}$$

where

$$[K_e] = k\pi.\int_0^1\int_0^1 \left([B]^T.[D].[B]\right).|J|.r.d\xi.d\eta.d\theta \tag{33}$$

is the element's stiffness matrix, and

$$\begin{aligned} [B] &= \left\lfloor\bar{d}\right\rfloor.[N] && (34a)\\ &= \left[\bar{d}\right].\left[[N_1],[N_2],\ldots,[N_i],\ldots,[N_{(p+1)(q+1)}]\right]^T && (34b)\\ &= \left[[B_1],[B_2],\ldots,[B_i],\ldots,[B_{(p+1)(q+1)}]\right]^T && (34c) \end{aligned}$$

Substituting Eq. 34c into Eq. 33, the element's stiffness matrix can be written, as

$$[K_e] = k\pi\int_0^1\int_0^1\sum_{i=1}^{p+1}\sum_{j=1}^{q+1}\left([B_i]^T.[D].[B_j]\right).r.|J|\,d\xi.d\eta \tag{35}$$

2.3.4 Mass Matrix

The kinetic energy can be written

$$\begin{aligned} T(t) &= \frac{1}{2}\int_{R_i}^{R_e}\int_0^H\int_O^{2\pi}\rho.\left\{\dot{\bar{\delta}}\right\}^T.[\theta_n]^T.[\theta_n].\left\{\dot{\bar{\delta}}\right\}.r.dr.dz.d\theta && (36a)\\ &= \frac{1}{2}\int_0^1\int_0^1\rho.\left\{\dot{\bar{\delta}}\right\}^T.\left(\int_O^{2\pi}[\theta_n]^T.[\theta_n].d\theta\right).\left\{\dot{\bar{\delta}}\right\}|J|.r.d\xi.d\eta && (36b)\\ &= \frac{k\pi}{2}\int_0^1\int_0^1\rho.\{\dot{q}\}^T.[N]^T.[N].\{\dot{q}\}.|J|.r.d\xi.d\eta && (36c)\\ &= \frac{1}{2}\{\dot{q}\}^T.\left(k\pi.\int_0^1\int_0^1\rho.[N]^T.[N].|J|.r.d\xi.d\eta\right).\{\dot{q}\} && (36d)\\ &= \frac{1}{2}\{\dot{q}\}^T.[M_e].\{\dot{q}\} && (36e) \end{aligned}$$

$$[M_e] = k\pi . \int_0^1 \int_0^1 \rho . [N]^T . [N] . |J| . r . d\xi . d\eta \tag{37a}$$

$$= k\pi . \int_0^1 \int_0^1 \rho . \sum_{i=1}^{p+1} \sum_{j=1}^{q+1} [N_i]^T . [N_j] |J| . r . d\xi . d\eta \tag{37b}$$

is the element's mass matrix.

2.3.5 Numerical Integration

The double integral appearing in the forms of the mass and stiffness matrices results in a numerical integration. For its implementation, one uses the Gauss quadrature expressed by

$$\int_0^1 f(x)\, d(x) = \sum_{i=1}^{N_{\text{int}}} W_i . f(x_i) \tag{38}$$

Where N_{int}, is the integration points number

After testing several integration points numbers, the number which is a compromise between the computing time and the precision is

$$N_{int} = p + 2 \tag{39}$$

Then to optimize calculations, the integration points number increase automatically with the interpolation polynomial degree.

3 Results and Discussions

The convergence and comparison studies must be carried out to ensure the reliability of the results. The vibration frequency ω is expressed in terms of the frequency parameter.

$$\Omega = \omega \sqrt{\frac{2(1+v)}{E}} \tag{40}$$

In this study, the Poisson's ratio, the Young modulus and the density takes respectively the values $\nu = 0.3$, E = 2 10^{11} KPa and ρ = 7830 Kg/m^3.

3.1 Convergence

The bi-hierarchical finite element is used for the first time, to study the free vibration of a very thin cylindrical shell with free boundary conditions. The external and internal radius are respectively R_e=1m and R_i=0.99m, the shell height is H=2m. Table 2 shows the convergence study of the first six modes with an increasing of the two hierarchical mode numbers p and q

following respectively the radius and the axis directions for two and four elements. The results are compared with those of the boundary collocation method [4] and those of ANSYS (20 harmonic and axisymmetric structural element solid with eight nodes). For the two idealization (Table 2), two and four elements, an accuracy of three digits after the comma is reached for the first two modes with p=2 and q=2.

For modes 3, 4, 5; the convergence is reached for p=6 and q=3 for a 2 elements model, and for p=4 and q=2 for a 4 elements model. The sixth mode reaches the convergence for p=8 and q=3 for 2 elements, and p=6 and q=2 for 4 elements. It is apparent that by increasing the number of elements, the hierarchical mode numbers p and q necessary to reach convergence are smaller, but the degrees of freedom number becomes more important. Indeed for mode 6 this number is of 300 for 4 elements whereas it is only of 189 for 2 elements. The matrices size is smaller if one increases p and q rather than the elements number. Table 2 shows that the number of degrees of freedom can be easily decreased by modifying the values of p and q according to the shell geometry.

3.2 Validation

In order to verify the accuracy of the bi-hierarchical finite element for solving the vibration of shells of revolution, a comparison study is conducted for different shells. A thick and a very thin cylindrical shells, a hollow cylindrical shell with varying thickness and a very thin plate. The results are compared with those of the boundary collocation method BCM, [4] and with those obtained by ANSYS where the harmonic and axisymmetric structural element solid with eight nodes is used.

The comparison of the frequency parameters Ω with those of the boundary collocation method [4] and ANSYS (32 harmonic and axisymmetric structural solid element with eight nodes) for a free thick cylindrical shell is given in table 3. The inner radius is R_i =1/3m, the outer radius is R_e =1m and the shell height is $H = 4/3m$. Considering that the results accuracy is quickly reached for a low number of elements if one increases the number of hierarchical modes, the shell is idealized by only four bi-hierarchical finite elements with the same hierarchical modes numbers p and q according to the axial and radial directions ($p = q = 8$). For this very thick cylindrical shell, the results given in table 3 are in good agreement with those of the two other methods, as well for the axisymmetric case as for the non-axisymmetric case. For high frequencies, results agree more with those of the BCM than with those of the ANSYS. The reason is that the warping of cross-sections is important and thus the interpolation polynomials degree must be larger to describe these modes. It is easily and automatically possible by using this bi-hierarchical finite element.

The second example is a very thin free cylindrical shell, idealized by four bi-hierarchical finite elements. The outer radius is R_e =1m; the inner radius is R_i =0.99m; and the height is H=2m. The hierarchical mode number along the shell axis is q=8 and that following the radius is p=4. The comparison results with those of the BCM [4] and those of ANSYS (20 elements) are given

Table 2: Convergence and Comparison Study of Frequency Parameter Ω For a Free Cylindrical Shell (R_e =1m, R_i =0.99m, H=2)

Element number	**q**	**p**	**DOF**	**Modes number**					
				1	**2**	**3**	**4**	**5**	**6**
2 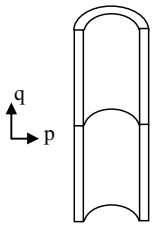	1	1	18	0.014	0.018	1.923	1.930	3.012	4.007
	2	1	30	0.014	0.018	1057	1.347	1.882	2.614
	2	2	45	0.013	0.017	1.057	1.346	1.882	2.614
	4	2	81	0.013	0.017	0.996	1.300	1.463	1.561
	4	3	108	0.013	0.017	0.996	1.300	1.463	1.561
	6	3	156	0.013	0.017	0.996	1.300	1.461	1.531
	8	3	189	0.013	0.017	0.996	1.300	1.461	1.530
	BCM			0.013	0.017	0.996	1.300	1.465	1.529
	ANSYS			0.013	0.017	0.996	1.303	1.463	1.533
4 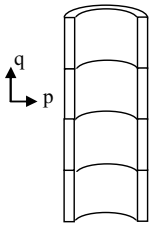	1	1	30	0.014	0.018	1.318	1.851	2.724	2.939
	2	1	54	0.014	0.018	0.998	1.310	1.529	1.576
	2	2	81	0.013	0.017	0.998	1.309	1.526	1.571
	4	2	153	0.013	0.017	0.996	1.300	1.461	1.531
	4	3	204	0.013	0.017	0.996	1.300	1.461	1.531
	6	3	300	0.013	0.017	0.996	1.300	1.461	1.530
	8	3	396	0.013	0.017	0.996	1.300	1.461	1.530
	BCM			0.013	0.017	0.996	1.300	1.465	1.529
	ANSYS			0.013	0.017	0.996	1.303	1.463	1.533

in table 4. The results are in perfect agreement with those of the BCM and those of ANSYS.

In the third example, a thick free hollow cylindrical shell with varying thickness is considered. Along the axis, the inner radius is R_i =0.6m and the outer radius is varying from R_e =0,8m at the edges, to R_e =1m at the middle height. The height is H =2m. The shell being thick, one takes the same hierarchical modes numbers ($p = q = 8$). Each half cylindrical shell is idealized by one bi-hierarchical finite element. Comparison of results with those of the BCM [4] and those of ANSYS (16 elements) are given in table 5. The same observation is made for the two other examples. The results agree very well with those of the BCM and those of ANSYS. This agreement illustrates the power of this element. Finally, to verify the accuracy of the bi-hierarchical finite element in solving the vibration of flattened shells of revolution, a very thin free circular plate is considered. The plate is idealized by two bi-hierarchical finite elements. The radius is R =1m and the thickness is H =0.05m. The hierarchical modes number along the shell thickness is q=3 and that following the radius is p=12. The comparison of results with those of the BCM [4] and those of ANSYS (20 elements) given in table 6, are in perfect agreement.

Table 3: Comparison of Frequency Parameters Ω for a Free Thick Cylindrical Shell (R_e=1m, R_i=1/3m, H=4/3,p=8,q=8)

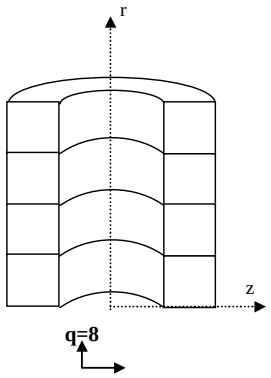

		Modes number					
circumferential wave number	**Method**	**1**	**2**	**3**	**4**	**5**	**6**
0	**Present**	2.298	2.512	3.237	4.138	4.502	6.352
	BCM	2.299	2.513	3.237	4.137	4.500	6.347
	ANSYS	2.300	2.514	3.239	4.141	4.508	6.368
1	**Present**	2.124	2.716	3.305	3.448	3.892	4.645
	BCM	2.123	2.716	3.304	3.447	3.89	4.645
	ANSYS	2.125	2.718	3.307	3.452	3.895	4.65
2	**Present**	1.371	1.444	3.142	3.143	4.195	4.626
	BCM	1.371	1.441	3.139	3.140	4.194	4.622
	ANSYS	1.370	1.442	3.142	3.143	4.199	4.630
3	**Present**	2.820	3.079	3.762	4.285	5.531	5.716
	BCM	2.818	3.071	3.758	4.279	5.526	5.711
	ANSYS	2.818	3.074	3.761	4.286	5.538	5.727
4	**Present**	4.068	4.401	4.686	5.404	6.514	6.585
	BCM	4.069	4.396	4.680	5.397	6.508	6.580
	ANSYS	4.070	4.401	4.686	5.407	6.525	6.598

3.3 Applications

The frequency parameter variation versus the circumferential wave number is carried out by using this element to idealize three shells of revolution. A very thin cylindrical shell (see Fig. 5), (height =2, thickness =0.01), a thick hollow cylindrical shell with linearly varying thickness (see Fig. 8) and a cylindrical shell of linearly varying thickness with a bottom plate like a storage tank (see Fig. 11). Along the axis, the inner radius is R_i =0.6m and the outer radius is varying from R_e =0.8m at the edges to R_e =1m at the middle height. The height is H =2m. The three shells are considered for the two cases, free base and clamped base. The vibration characteristics of a cylindrical shell could be evaluated by observing the radial deformation. Fig. 4 shows the circumferential node patterns of a cylindrical shell, n being the circumferential wave number. For $n = 0$, the circumferential nodal pattern is a circle, indicating that this mode is an extensional mode referred to as breathing type mode. $n = 1$ indicates two crossings between the deformed and original shapes, $n = 2$ indicates four crossings. The lowest frequency does not occur at the lowest values of n. For example, for the thin clamped base cylindrical shell, the lowest frequency occurs when $n = 4$, for the other examples this frequency occurs when $n = 2$. This phenomenon can be explained by considering the strain energy of the middle surface under both bending and stretching [7].

The figures, 6, 7, 9, 10, 12 and 13 shows the variation of the frequency parameters against the circumferential wave number given by six curves. The first curve indicated by $m = 1$ is corresponding to the first lowest frequency parameter, the second curve (m =2) to the second lowest one etc. Fig. 6 shows for the free cylindrical shell, that for $n = 0$ (the axisymmetric case),

Table 4: Comparison of Frequency Parameters Ω For a Free Thin Cylindrical Shell (R_e =1m, R_i=0.99m, H=2m, p=4, q=8)

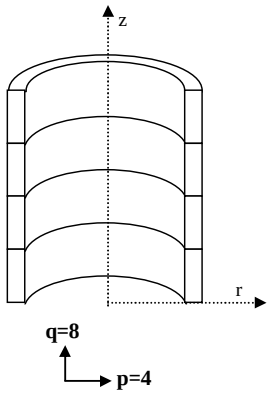

		Modes number					
circumferential wave number	**Method**	**1**	**2**	**3**	**4**	**5**	**6**
0	**Present**	1.576	1.613	1.618	1.620	1.625	1.636
	BCM	1.576	1.613	1.618	1.618	1.630	1.639
	ANSYS	1.577	1.613	1.618	1.621	1.625	1.637
1	**Present**	1.248	1.414	1.545	1.583	1.611	1.641
	BCM	1.248	1.414	1.544	1.587	1.612	1.658
	ANSYS	1.250	1.416	1.546	1.584	1.613	1.643
2	**Present**	0.013	0.017	0.995	1.300	1.461	1.530
	BCM	0.013	0.022	0.996	1.297	1.465	1.529
	ANSYS	0.013	0.017	1.000	1.303	1.463	1.533
3	**Present**	0.037	0.044	0.660	1.059	1.292	1.422
	BCM	0.037	0.048	0.662	1.056	1.297	1.419
	ANSYS	0.037	0.044	0.665	1.063	1.295	1.425
4	**Present**	0.071	0.079	0.453	0.838	1.114	1.294
	BCM	0.072	0.083	0.458	0.835	1.121	1.291
	ANSYS	0.071	0.079	0.457	0.843	1.118	1.298

Table 5: Comparison of Frequency Parameters Ω For a Free Hollow Cylindrical Shell of Varying Thickness (R_e =Varying, R_i=0.6m, H=2m, p=8,q=8)

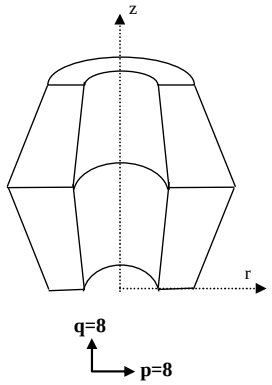

		Modes number					
circumferential wave number	**Method**	**1**	**2**	**3**	**4**	**5**	**6**
0	**Present**	2.006	2.193	2.366	2.844	3.273	3.880
	BCM	2.007	2.195	2.367	2.839	3.279	3.896
	ANSYS	2.007	2.193	2.367	2.846	3.275	3.889
1	**Present**	1.629	1.996	2.518	2.832	3.370	3.382
	BCM	1.627	2.002	2.518	2.835	3.370	3.384
	ANSYS	1.629	1.997	2.519	2.839	3.373	3.386
2	**Present**	0.644	0.761	1.853	2.466	2.967	3.309
	BCM	0.646	0.760	1.861	2.464	2.963	3.308
	ANSYS	0.644	0.761	1.855	2.468	2.976	3.312
3	**Present**	1.641	1.762	2.444	3.356	3.767	4.228
	BCM	1.641	1.755	2.449	3.348	3.761	4.228
	ANSYS	1.642	1.763	2.448	3.365	3.774	4.239
4	**Present**	2.811	2.904	3.451	4.229	4.996	5.163
	BCM	2.811	2.890	3.453	4.214	4.991	5.166
	ANSYS	2.815	2.908	3.458	2.242	5.009	5.188

the frequency parameters are almost the same. Starting from a number of circumferential wave equal to 1 (non-axisymmetric case) the frequency parameters decrease gradually except for the first two lowest ones (corresponding to $m = 1$ and $m = 2$) which decrease quickly to the value 2

Table 6: Comparison of Frequency Parameters Ω for a Free Thin Circular Plate (Thickness =0.05m, Radius =2m, p=12, q= 3)

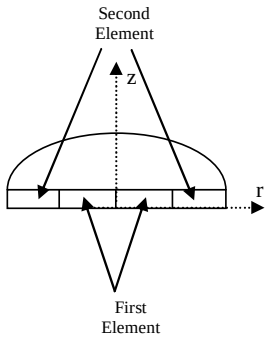

		Modes number					
circumferential wave number	**Method**	**1**	**2**	**3**	**4**	**5**	**6**
0	**Present**	0.219	0.924	2.070	3.463	3.611	9.104
	BCM	0.219	0.923	2.066	3.463	3.595	9.104
	ANSYS	0.219	0.924	2.070	3.463	3.610	9.108
1	**Present**	0.495	1.424	2.734	2.772	4.493	5.964
	BCM	0.494	1.419	2.734	2.761	4.464	5.964
	ANSYS	0.495	1.425	2.734	2.774	4.493	5.965
2	**Present**	0.130	0.846	1.990	2.345	3.532	4.244
	BCM	0.136	0.840	1.977	2.345	3.506	4.244
	ANSYS	0.130	0.846	1.990	2.345	3.533	4.245
3	**Present**	0.301	1.262	2.613	3.601	4.340	5.834
	BCM	0.308	1.251	2.590	3.601	4.296	5.834
	ANSYS	0.300	1.261	2.612	3.601	4.335	5.835
4	**Present**	0.525	1.736	3.287	4.689	5.194	7.437
	BCM	0.532	1.718	3.253	4.689	5.126	7.438
	ANSYS	0.525	1.734	3.285	4.689	5.180	7.439

then increase gradually. The cylindrical shell with clamped edge (see Fig. 7), is a similar case except for the curves corresponding to $m = 1$ and $m = 2$ whose frequency parameters increase between values 0 and 1 of the circumferential wave number then decrease gradually. For the hollow cylindrical shell and the composed shell (cylindrical shell and plate), the lowest frequency occurs at $n = 2$ for the two cases, free base (see Fig. 9 and Fig. 12) and clamped base (see Fig. 10 and Fig. 13). The only difference between the two cases is that for $n = 0$ and for $n = 2$, the gap between the frequency values is slightly more important for the clamped base case than for the free base one. Otherwise, for the two cases of the two shells, the frequency parameters increase linearly from a number of circumferential waves equal to 2.

4 Conclusion

The bi-hierarchical finite element presented in this study is able to give accurate frequencies for shells of revolution of linearly varying thickness. The results show clearly that this element can be easily used for the extreme cases of very thin or very thick shells of revolution. With this element one is not constrained any more to have the same number of hierarchical modes in the two main directions of the radial and axial shells of revolution. Indeed, if the shapes and dimensions change (thick or thin shells) the hierarchical mode number can change very easily. This element can also be used to idealize a composed shell, plate linked to cylindrical shell for example. Finally this bi-hierarchical finite element allows triple increase in the accuracy, finite elements number, and radial and axial hierarchical modes numbers.

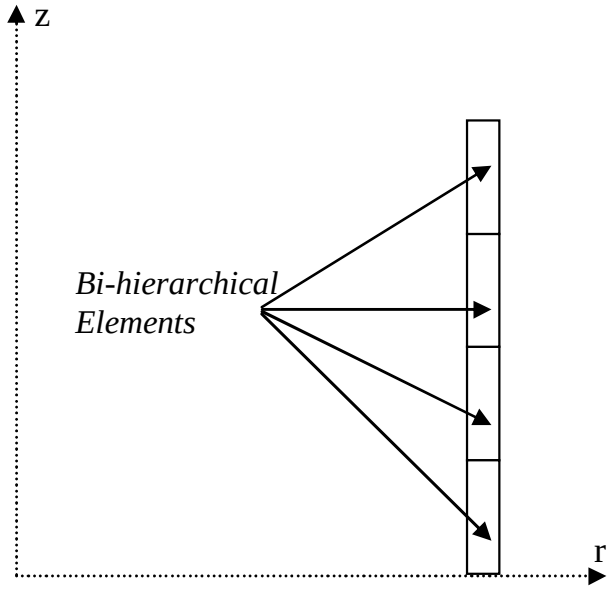

Figure 5: Idealization of the cylindrical thin shell

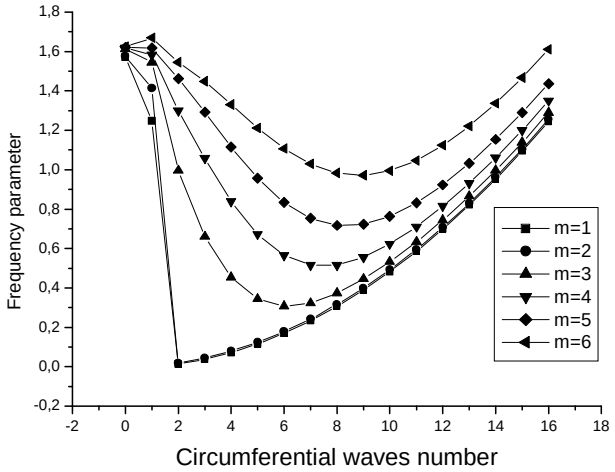

Figure 6: Frequency parameters variation versus the circumferential wave number of a very thin free-free cylindrical shell (thickness =0.01, height =2m, p=2, q= 12).

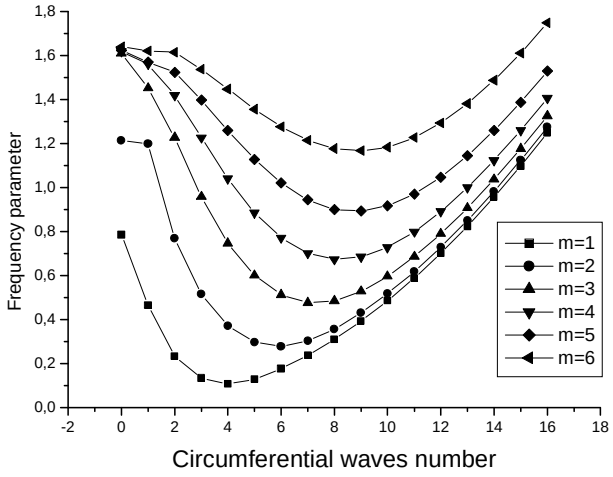

Figure 7: Frequency parameters variation versus the circumferential wave number base of a free-clamped very thin cylindrical shell (Thickness =0.01m, height =2m, p=2, q= 12).

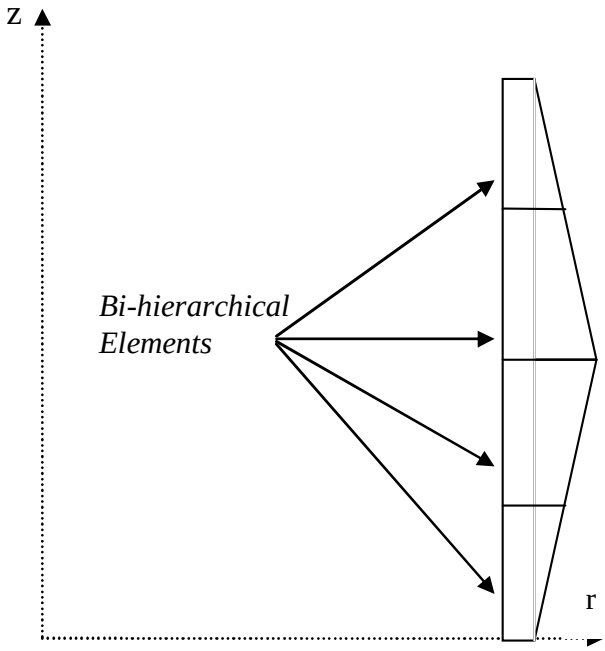

Figure 8: Idealization of the thick hollow cylindrical shell with linearly varying thickness

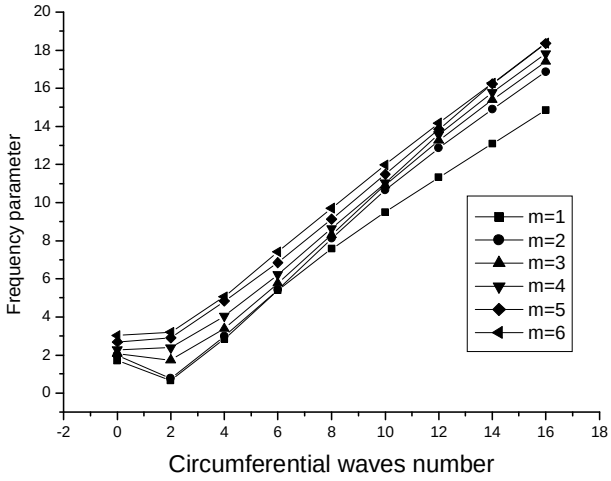

Figure 9: Frequency parameters variation versus the circumferential wave number of a free- free hollow Cylindrical Shell Of Varying Thickness (R_e =Varying, R_i= 0.6m, H =2m, p=8, q=8).

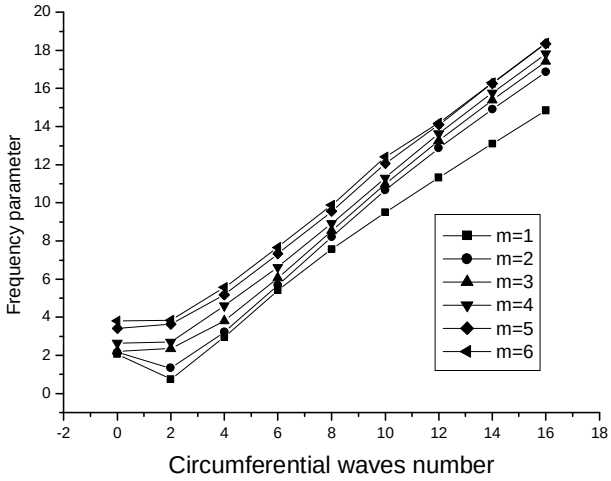

Figure 10: Frequency parameters variation versus the circumferential wave number of a free-clamped hollow Cylindrical Shell Of Varying Thickness (R_e =Varying, R_i= 0.6m, H =2m, p=8, q=8).

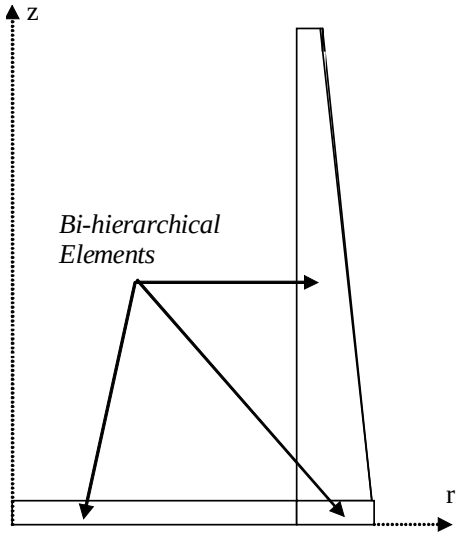

Figure 11: cylindrical shell of linearly varying thickness with a bottom plate

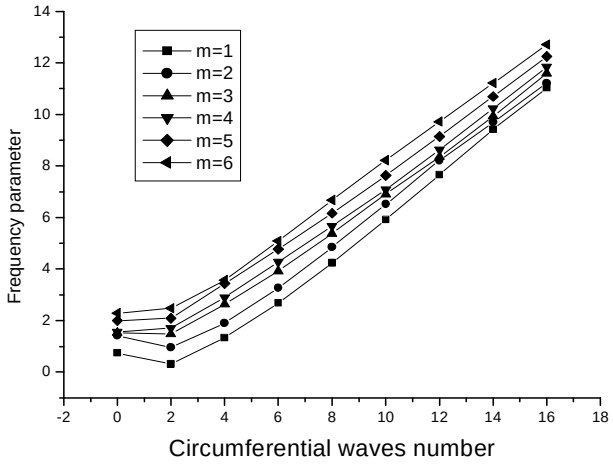

Figure 12: Frequency parameters variation versus the circumferential wave number of a cylindrical shell of linearly varying thickness with a free bottom plate.

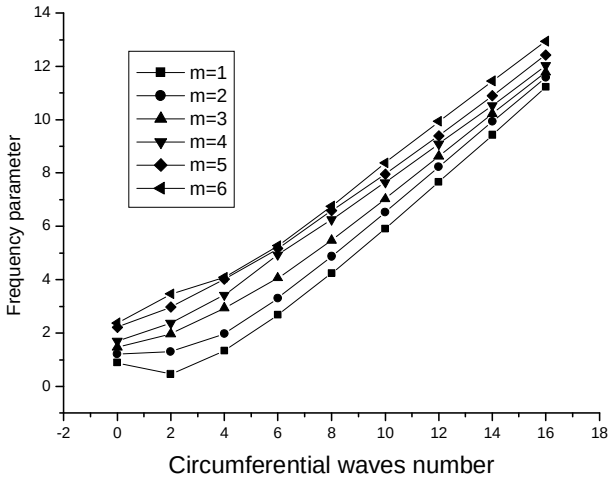

Figure 13: Frequency parameters variation versus the circumferential wave number of a cylindrical shell of linearly varying thickness with a clamped bottom plate.

References

[1] I. Babuska and B. Szabo. On the rates of convergence of the finite element method. *Int. J. Num. Meth. Engng.*, 18(3):323–341, 1982.

[2] J.L. Batoz and G. Dhatt. *Modélisation des structures par éléments finis*, volume 3. Presses Université Laval, 1992.

[3] A. Houmat. Three dimensional hierarchical finite element free vibration analysis of annular sector plates. *Journal of Sound and Vibrations*, 276(1-2):181–193, 2004.

[4] A. Houmat and J.R. Hutchinson. Free vibration of bodies of revolution by boundary collocation. *Journal of Sound and Vibrations*, 171(1):35–48, 1994.

[5] A.S. Kairov. Free vibrations of a conical shell of slightly varying thickness with annular strengthening. *Journal of Mathematical Sciences*, 60(1):1573–3374, 1992.

[6] J.H. Kang and A.W. Leissa. Free vibration of thick complete conical shells of revolution from a three-dimensional theory. *Journal of Applied Mechanics*, 72(5):797–800, 2005.

[7] H. Kraus. *Thin elastic shells*. John Wiley, 1967.

[8] W. Leissa. Three-dimensional vibration analysis of thick shells of revolution. *Journal of Engineering Mechanics*, 125(12):1365–1371, 1999.

[9] H.J. Shim and J.H. Kang. Free vibration of solid and hollow hemi-ellipsoids of revolution from a three-dimensional theory. *Int. Journal of Engineering Science*, 42(17-18):1793–1815, 2004.

[10] K. Suzuki and A.W. Leissa. Free vibrations of noncicular cylindrical shells having circumferentially varying thickness. *Journal of applied mechanics*, 52(1):149–154, 1985.

[11] B.A. Szabo. The use of a priori estimates in engineering computations. *Comp. Meth. Appli. Mech. Engng.*, 82(1-3):139–154, 1990.

[12] B.A. Szabo and I. Babuska. *Finite element analysis*. John Willey, 1991.

[13] D.Y. Tan. Free vibration analysis of shells of revolution. *Journal of Sound and Vibrations*, 213(1):15–33, 1998.

[14] P.G. Young. Application of a three-dimensional shell theory to the free vibration of shells arbitrarily deep in one direction. *Journal of Sound and Vibrations*, 238(2):257–269, 2000.